

Preliminary Crystallographic Characterization of Ricin Agglutinin

E.C. Sweeney,¹ A.G. Tonevitsky,² D.E. Temiakov,² I.I. Agapov,² S. Saward,¹ and R.A. Palmer^{1*}

¹Department of Crystallography, Birkbeck College, University of London, London, United Kingdom

²Institute of Genetics of Micro-organisms, Moscow, Russia

ABSTRACT The quaternary structure of ricin agglutinin (RCA) has been determined by x-ray crystallography. The refined structure of ricin proved to be a successful search model using the molecular replacement method of phase determination. RCA forms an elongated molecule of dimensions $120 \text{ \AA} \times 60 \text{ \AA} \times 40 \text{ \AA}$ with two A chains at the center and a B chain at each end. The A chains are covalently associated via a disulfide bridge between Cys 156 of both chains. Additional contacts at residues 114–115 stabilize the dimer interface. The covalent association of RCAA chains was confirmed by gel filtration under reducing and nonreducing conditions. *Proteins* 28:586–589, 1997.

© 1997 Wiley-Liss, Inc.

Key words: ribosome inactivating protein; RIP; ricin; dimer formation; molecular replacement

Both ricin and RCA belong to the type II RIP family.¹ These proteins are also classified as lectins, as they are able to bind specific sugars. Ricin has an affinity for galactose (gal) and *N*-acetylgalactosamine (galNAc) containing oligosaccharides,² while RCA recognizes mainly galactose-containing sugars.³ Both proteins consist of a toxic subunit, the A chain, and a sugar-binding subunit, the B chain, linked by a disulfide bridge. RCA consists of two A chains each of molecular weight 29,500 Da and two B chains of 37,000 Da, while ricin consists of one A chain and one B chain. RCA and ricin are the product of distinct genes, and it has been suggested that the ricin gene probably evolved first, then duplicated to give rise to two genes, one that continued to code for ricin, and the other that underwent evolutionary mutations to produce RCA.⁴ The RCA gene produces the AB heterodimer, which undergoes posttranslational modification, joining up with another molecule to form the [BAAB] dimer.⁵ Amino acid sequence information on this protein shows that the A chain of RCA is 93% homologous to ricin, while the B chain has 84% homology.

Crystals of RCA were grown by using the hanging drop vapor diffusion method as previously described for MLI.⁶ A complete x-ray intensity dataset to 3.60 \AA

resolution was collected on the RCA crystal in-house on a 180-mm Mar Research Image Plate Detector ($\lambda = 1.54178$), using a rotating anode source with 40 kV and 96 mA. These data were indexed by using the DENZO software.⁷ This indicated a trigonal unit cell, which refined to $a = b = 100.05 \text{ \AA}$, $c = 212.58 \text{ \AA}$, and one RCA molecule per asymmetric unit, including 69% solvent. The x-ray intensity data were scaled and merged by using the CCP4 suite of programs.⁸ A total of 13,235 unique reflections were recorded, giving a dataset 96% complete for $d_{\min} = 3.6 \text{ \AA}$, with an R_{merge} of 10.0%.

The molecular replacement method was carried out with the program AMoRe,⁹ by using the ricin structure of Monfort and colleagues¹⁰ as the search model. Although ricin is only half the size of RCA, it was expected to yield a solution due to the high amino acid sequence homology. The search-model Patterson maps were calculated in the resolution range 3.6 \AA – 20.0 \AA by placing ricin into an orthogonal cell of P1 symmetry with unit cell parameters $110 \text{ \AA} \times 85 \text{ \AA} \times 65 \text{ \AA}$. The rotation function was stepped over 2.5° and the radii of integration varied between 15 and 30 \AA . An overall artificial temperature factor of $\exp(-B \sin^2 \theta/\lambda^2)$, where $B = -20 \text{ \AA}^2$ was applied to provide sharpening of the Patterson function. In space group P3₂ two translation function solutions were found with peak heights in the range 5.2σ to 5.0σ above the highest noise peak having R factors of 44% and correlation coefficients of 55%, following the rigid body refinement protocol of AMoRe. To check the validity of this solution, calculation of the rotation and translation function was

Abbreviations: RCA, ricin agglutinin; RTA, ricin A-chain; RTB, ricin B-chain; RIP, ribosome inactivating protein; RMS, root mean square; DTT, dithiothreitol; merging R factor, $\sum_i (\sum_j |F_o|_i^2 - (\sum_j |F_o|_j^2)_{av}) / \sum_h (\sum_i |F_o|_i^2)_{av}$, provides an overall agreement index between reflections and symmetry equivalents measured more than once. R factor, $\sum_i |F_o|_i - |F_c| / \sum_i |F_o|_i$ over unique hkl data; correlation coefficient $[\sum_h |\Delta| F_o| \Delta| F_c|] \times [\sum_h (\Delta| F_o|)^2] \times [\sum_h (\Delta| F_c|)^2]^{-1/2}$, where $\Delta| F_h|$ stands for $|F_h| - |F_h|_{av}$ corresponding to the highest peaks of the translation function; gal, galactose; gal NAC, *N*-acetyl galactosamine.

*Correspondence to: R.A. Palmer, Department of Crystallography, Birkbeck College, University of London, London WC1E 7HX, United Kingdom.

Received 19 June 1996; Accepted 8 November 1996

repeated five times, with the starting model in different orientations, varying the resolution range, model cell parameters, and radii of integration. These solutions proved to be consistent. Symmetry-related molecules were generated, and the unit cell packing was examined by using the MOLPACK program.¹¹ No stereochemical clashes were observed, and the packing of the model in the crystal clearly demonstrates the interface region between the two molecules involved in the RCA mode of dimerization. Electron density maps ($|F_o| - |F_c|$) and $(2|F_o| - |F_c|)$ were computed within the resolution range 3.6 Å to 10 Å by using phases calculated from the refined model and displayed by using the graphics program O.¹² The initial $(2|F_o| - |F_c|)$ electron density map, contoured to 1.25 times the RMS density level, showed good connectivity for the polypeptide chains, thus confirming the validity of the molecular replacement solution. No molecular replacement solution was found in space group P3₁.

In order to confirm the presence of a disulfide bond between the two A chains of RCA, the retention times of the molecule in its native and reduced form were analyzed on Superdex-75HR 10/30. Ricin was used as a control protein. Samples were applied at a concentration of 1 mg/ml in PBS pH 7.4 with 20 mM lactose and a flow rate of 1 ml/min. The protein was exposed to mercaptoethanol and varying concentrations of DTT between 0.5 and 20 mM.

The RCA molecules pack as BAAB dimers (Fig. 1) around 3₂ screw axes in the crystallographic unit cell. The tertiary structure of RCA closely resembles that of ricin, both proteins being composed of an A chain and a B chain joined by a disulfide bridge. The RMS deviation calculated for all C α atoms of RCA and ricin is 0.9 Å. Secondary structural features are mostly conserved between the two proteins, apart from small changes due to evolutionary mutations in the amino acid sequence. The A chains are identical in all but 18 positions. Key active-site residues of the A chain were identified and found to be conserved between both proteins. The most striking evolutionary change between ricin and RCA is the exchange of Gly on ricin for Cys 156 on the A chain of RCA.⁵ This residue is located on a hydrophilic loop between two major helices, D (residues 141–152) and E (residues 161–180).¹³ It can be seen from the crystallographic structure analysis that this loop extends out from the surface of the molecule and that the Cys forms a disulfide bridge with the A chain of an adjacent molecule (Fig. 2). The second point of close contact between the two A chains occurs on a loop between the two helices, B (residues 99–104) and C (residues 122–127), which also extends out from the surface of the protein to interact with an adjacent molecule (Fig. 3). Two residues on this loop Ser114 and Phe115 of RCA add further support to the dimer interface.

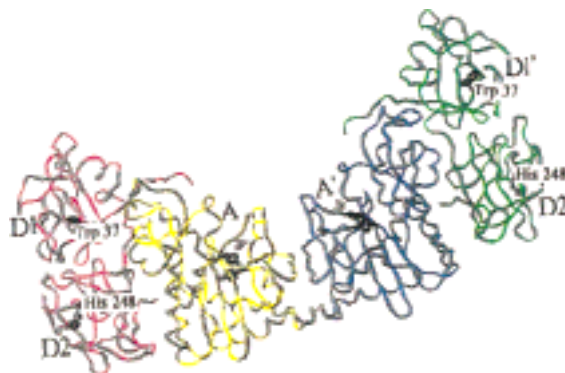


Fig. 1. Structural features of the RCA dimer: S—S indicates the disulfide bond between the A subunits (A and A') of the AB heterodimers. Important active site regions of the A subunits containing Tyr80 and Tyr124 are indicated with an asterisk. The Tyr37 residues at the sugar binding sites on domain 1 (D1 and D1') are indicated. The His248 residues associated with loss of sugar binding activity on domain 2 (D2 and D2') are also shown.

These residues are replaced by Arg114 and Tyr115, respectively, in ricin.

The covalent association of RCA A chains was confirmed by gel filtration (Fig. 4). Peak A represents RCA in the nonreduced form eluting as a 120,000 Mr protein. Peak B was RCA in 0.5 mM DTT reducing agent eluting mainly at 120,000, with a smaller peak indicating the presence of a 60,000 monomer (not shown). This proves that at 0.5 mM DTT, 10% of the A—A disulfide bonds were reduced. Peak C shows that in 5 mM DTT 52% of the A—A bridges were reduced. The smaller peak c shows that some of the A—B disulfide bridges are also reduced. Peak D demonstrated that in 20 mM DTT, 80% of the protein eluted in the [AB] monomeric form, while the remaining 20% of the protein remained intact (not shown). Peak E represents complete reduction of the RCA homodimer to the AB monomeric form in the presence of 50 mM DTT. The smaller peak e shows that a significant number of A—B disulfide bridges are also reduced in this concentration of DTT.

These results confirm the crystallographic finding that a disulfide bond exists between the two ricinlike monomers and that reduction of this bond is dependent on the concentration of the reducing agent added. The separation of individual A and B chains was also observed under these conditions, although, due to additional strong hydrophobic contact between these chains, the disulfide bridge was more resistant to reduction. In order to separate the A and B chains, in addition to reducing agent, strongly alkaline buffer is needed to abolish the hydrophobic contact that can hold the two chains together independent of the disulfide bond.

The B chain of RCA, like ricin, is a lectin composed of two structurally similar domains.² Domain 1 of

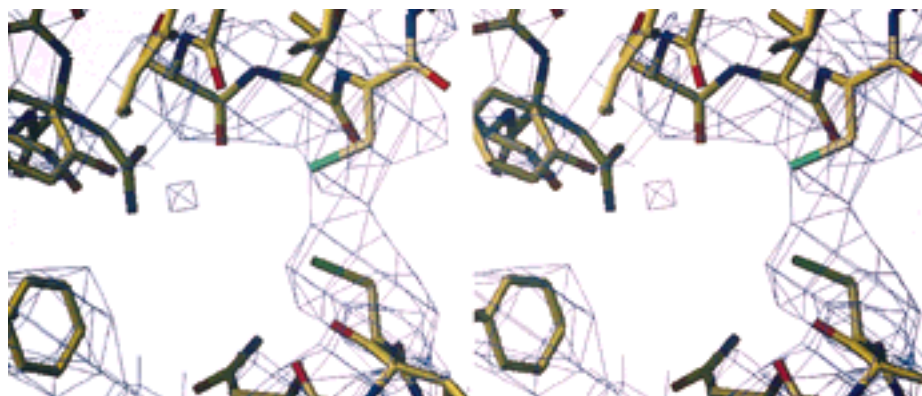


Fig. 2. The $(2|F_o| - |F_c|)$ electron density in the vicinity of the disulfide bridge between the two A chains is shown. The map was contoured at 1.25 times the RMS density level and displayed in stereo by using the program O.¹²

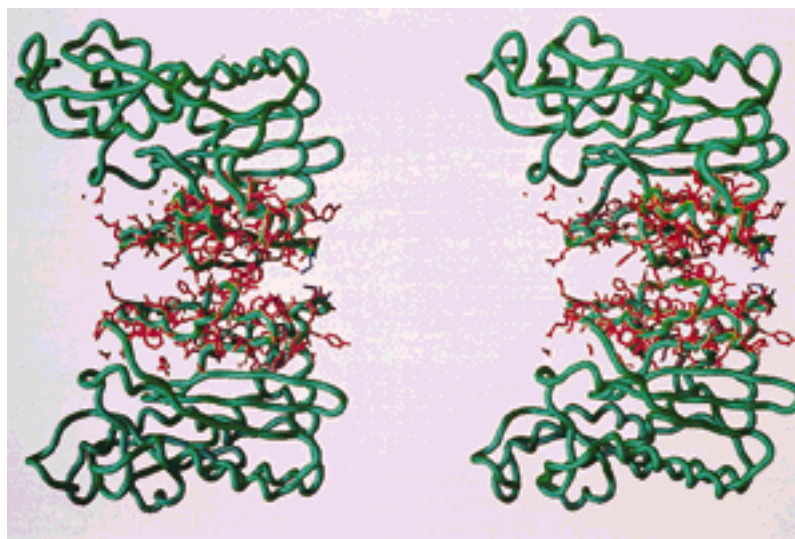


Fig. 3. Stereoview of the RCA dimer interface showing both A chains.

ricin binds to galactose, while domain 2 has an affinity for both galactose and *N*-acetylgalactosamine. The primary structure of the RCA B chain differs from ricin at 41 positions, but the most significant mutation of RCA is His248, replaced by Tyr in ricin, causing loss of sugar-binding activity at the high-affinity site of domain 2.¹⁴ RCA therefore retains two galactose-binding sites on each of the two B chain domain 1 subunits situated 100 Å apart. The difference in quaternary structure between RCA and ricin is therefore primarily as a result of three evolutionary mutations: Arg114 → Ser, Tyr115 → Phe, and Gly157 → Cys.

The B chains of these proteins are composed of two similar domains that appear to adopt a β -trefoil structure.¹⁵ In ricin both of these domains bind galactose in a pocket formed by residues Asp-Val-Arg

(22–24 in domain 1 and 234–236 in domain 2). The RCA molecule retains the domain 1 sugar-binding site of both B chains. Although Arg24 is replaced by Thr in the sugar-binding pocket, this mutation does not appear to affect galactose binding. A single mutation of Trp248 to His in RCA, however, causes loss of sugar-binding activity in domain 2.⁵ The agglutination potential of RCA is approximately 60 times greater than that of ricin in the presence of human group A erythrocytes.¹⁴ This difference is most probably a consequence of RCA dimerization. It is likely that the greater distance between domain 1 sugar-binding sites on RCA (100 Å) allows the molecule to more effectively bridge the gap between cell receptors.

All major active-site residues of the A chains were found to be conserved among these molecules, although RCA is only 1/100 times as toxic as ricin

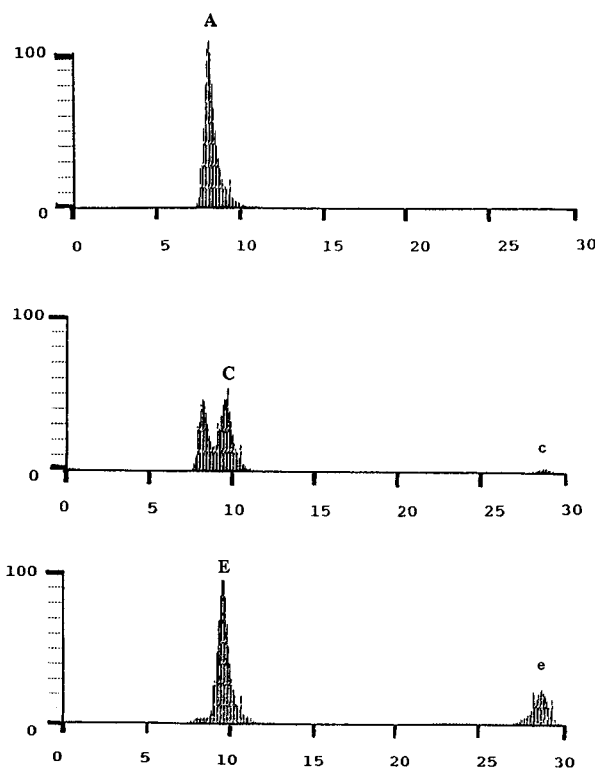


Fig. 4. Elution volumes of RCA and ricin in the presence of reducing agents. Peak A, native RCA, peak C, RCA in 5 mM DTT, peak E, RCA in 50 mM DTT.

tested on different cell lines. The differences in potency does not appear to be a consequence of dimerization, since the RCA [AB] monomer has the same cytotoxicity as the [BAAB] dimer (A.G. Tonevitsky, personal communication). Through the use of site-directed mutagenesis we plan to investigate whether galNAC binding to cell receptors plays a critical role in endocytic uptake for optimizing the cytotoxic effect.

ACKNOWLEDGMENTS

E.C.S. thanks the Medical Research Council for funding during the course of this work. A.G.T. thanks The Wellcome Trust International. We all thank the

MADAUS company of Cologne, Germany for useful discussions during the course of this work.

REFERENCES

1. Barbieri, L., Batteli, M.G., Stirpe, F. Ribosome inactivating proteins from plants. *BBA*. 1154:237–282, 1993.
2. Katzin, B.J., Collins, E.J., Robertus, J.D. Structure of ricin B-chain at 2.5 Å resolution. *Proteins* 10:251–259, 1991.
3. Baenziger, J., Fiete, D. Structural determination of *Ricinus communis* agglutinin and toxin specificity for oligosaccharides. *J. Biol. Chem.* 254:9795–9799, 1979.
3. Brunger, A.T., Krutowsky, A., Erickson, J. Slow cooling protocols for crystallographic refinement by simulated annealing. *Acta Crystallogr.* A46:585–593, 1990.
4. Ready, M., Wilson, K., Piatak, M., Robertus, J.D. Ricin-like plant toxins are evolutionarily related to single-chain ribosome inhibiting proteins from phytolacca. *J. Biol. Chem.* 259:15252–15256, 1984.
5. Roberts, L.M., Lamb, F.I., Pappin, D.J.C., Lord, J.M. The primary sequence of *Ricinus communis* agglutinin. *J. Biol. Chem.* 260:15682–15686, 1985.
6. Sweeney, E.C., Palmer, R.A., Pfuller, U. Crystallisation of the ribosome inactivating protein MLI from *Viscum album* (mistletoe) complexed with β -D-galactose. *J. Mol. Biol.* 234:1279–1281, 1993.
7. Otwinowski, Z. Oscillation data reduction program in data collection and processing. "Proceedings of the CCP4 Study Weekend, 29–30." Sawyer, L., Isaacs, N., Bailey, S. (eds.). Daresbury, U.K.: SERC Daresbury Laboratory, 1993:56–62.
8. CCP4 Protein Crystallography Programme Suite. CLRC, Daresbury Laboratory, UK.
9. Navaza, J. AMoRe: An automated package for molecular replacement. *Acta Cryst.* A50:157–163, 1994.
10. Monfort, W., Villafranca, J.E., Monzingo, A.F., Ernst, S.R., Katkin, B., Rutenber, E., Xuong, N.H., Hamlin, R., Robertus, J.D. The three dimensional structure of ricin at 2.8 Å. *J. Biol. Chem.* 262:5398–5403, 1987.
11. Wang, D., Driessen, H.P.C., Tickle, I.J. MOLPACK: Molecular graphics for studying the packing of protein molecules in the crystallographic unit cell. *J. Mol. Graph.* 9:28, 50–52, 1991.
12. Jones, T.A., Zou, Y.-J., Cowan, S.W., Kjegaard, M. Improved methods for building protein models in electron density maps and the location of errors in these models. *Acta Crystallogr.* A47:110–119, 1991.
13. Rutenber, E., Robertus, J.D. Structure of ricin A-chain at 2.5 Å resolution. *Proteins* 10:260–269, 1991.
14. Sphyris, N., Lord, J.M., Wales, R., Roberts, L.M. Mutational analysis of the ricinus lectin B-chains. *J. Biol. Chem.* 270:20292–20297, 1995.
15. Murzin, A.G., Lesk, A.M., Chothia, C. β -Trefold patterns of structure and sequence in the Kunitz inhibitors interleukins-1 β and 1 α and fibroblast growth factors. *J. Mol. Biol.* 223:531–543, 1992.